NANO LETTERS

Letter

pubs.acs.org/NanoLett

Effect of Elastic Strain Fluctuation on Atomic Layer Growth of Epitaxial Silicide in Si Nanowires by Point Contact Reactions

Yi-Chia Chou,*[,†] Wei Tang,[‡] Chien-Jyun Chiou,[†] Kai Chen,[§,∥] Andrew M. Minor,[§] and K. N. Tu[‡]

[†]Department of Electrophysics, National Chiao Tung University, Hsinchu 300, Taiwan

[‡]Department of Materials Science and Engineering, University of California Los Angeles, Los Angeles, California 90095, United States

[§]National Center for Electron Microscopy, Molecular Foundry, Lawrence Berkeley National Laboratory, Berkeley, California 94720, United States

[∥]Center for Advancing Materials Performance from the Nanoscale, State Key Laboratory for Mechanical Behavior of Materials, Xi'an Jiaotong University, Xi'an, China

Supporting Information

ABSTRACT: Effects of strain impact a range of applications involving mobility change in field-effect-transistors. We report the effect of strain fluctuation on epitaxial growth of $NiSi_2$ in a Si nanowire via point contact and atomic layer reactions, and we discuss the thermodynamic, kinetic, and mechanical implications. The generation and relaxation of strain shown by in situ TEM is periodic and in synchronization with the atomic layer reaction. The Si lattice at the epitaxial interface is under tensile strain, which enables a high solubility of supersaturated interstitial Ni atoms for homogeneous nucleation of an epitaxial atomic layer of the disilicide phase. The tensile strain is reduced locally during the incubation period of nucleation by the dissolution of supersaturated Ni atoms in the Si lattice but the strained-Si state returns once the atomic layer epitaxial growth of $NiSi_2$ occurs by consuming the supersaturated Ni.

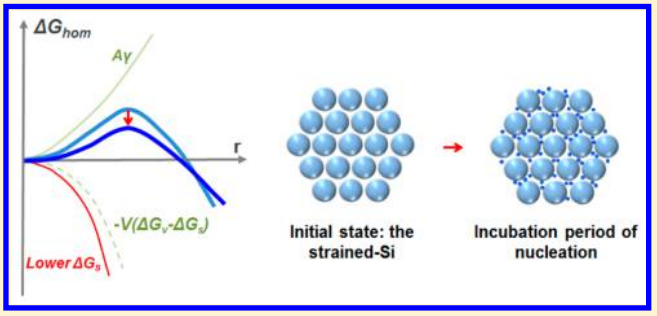

KEYWORDS: *Silicide, nanowire, strain, point contact reaction, nucleation*

On basis of the roadmap of miniaturization beyond the limit of Moore's law of the metal-oxide-semiconductor field-effect-transistors (MOSFETs) for Si chip technology in semiconductor industry, the growth fundamentals, precision controls, and applications of nanowires and quantum dots are critical for nanoelectronics, quantum computers, and biosensors.[1−5] It involves the developments of complex geometries, self-assembly techniques, and hybrid nanostructures allowing transistor scaling and optimization of the statics and performances of devices.[6−12] Metal silicides have been widely used as contacts, electrodes, and even short interconnects in very-large-scale-integration (VLSI) technology for Si industry even down to nanoscale.[13−16] Clearly, silicide is an essential building block in Si-based technology owing to the successful control of the formation of nanoscale silicides on Si, such as the salicide process,[17] and the outstanding physical properties.[18−21] The growth mechanism, and precision control of silicide thin films and nanowires formation, and the interface reactions where silicide acts as the catalyst have been reported.[22−26]

Silicide formation (such as NiSi, $NiSi_2$, $CoSi_2$ phases) in Si nanowires by point contact reaction occurs as Ni or Co atoms diffuse into Si nanowires via a point of contact at temperatures of 450 to 800 °C, and the Si transformed to silicide, atomic layer by atomic layer, with an incubation time of nucleation between every atomic layer growth.[27−29] The silicide phase formation in nanoscale has not been defined systematically, but a strong dependence on annealing temperature has been found,[27] where the sequence of formation is the same as in thin film reactions, for example, it forms Ni-rich phase at lower temperatures but Si-rich phase at higher temperatures. The mechanism of silicide phase transformation in Si nanowires is different from that of thin film silicide formation on Si wafers.[27,30] The main difference is the atomic layer reaction in nanowires because of the requirement of repeating events of homogeneous nucleation.[31] Homogeneous nucleation requires a large supersaturation, so it is initiated after the supersaturation level of metal solutes in Si nanowires is reached during the incubation period, however, the large dissolution causes volume change and results in the change of the strain level in a finite space of the nanowire or heterostructure with the confinement of native oxide on the nanowire surface.

We report here, during the incubation time, while waiting for achieving a supersaturation of Ni in the nanowire, mainly interstitials and possibly a very small amount of substitutional

Received: March 31, 2015
Revised: April 30, 2015
Published: May 12, 2015

DOI: 10.1021/acs.nanolett.5b01234
Nano Lett. 2015, 15, 4121−4128

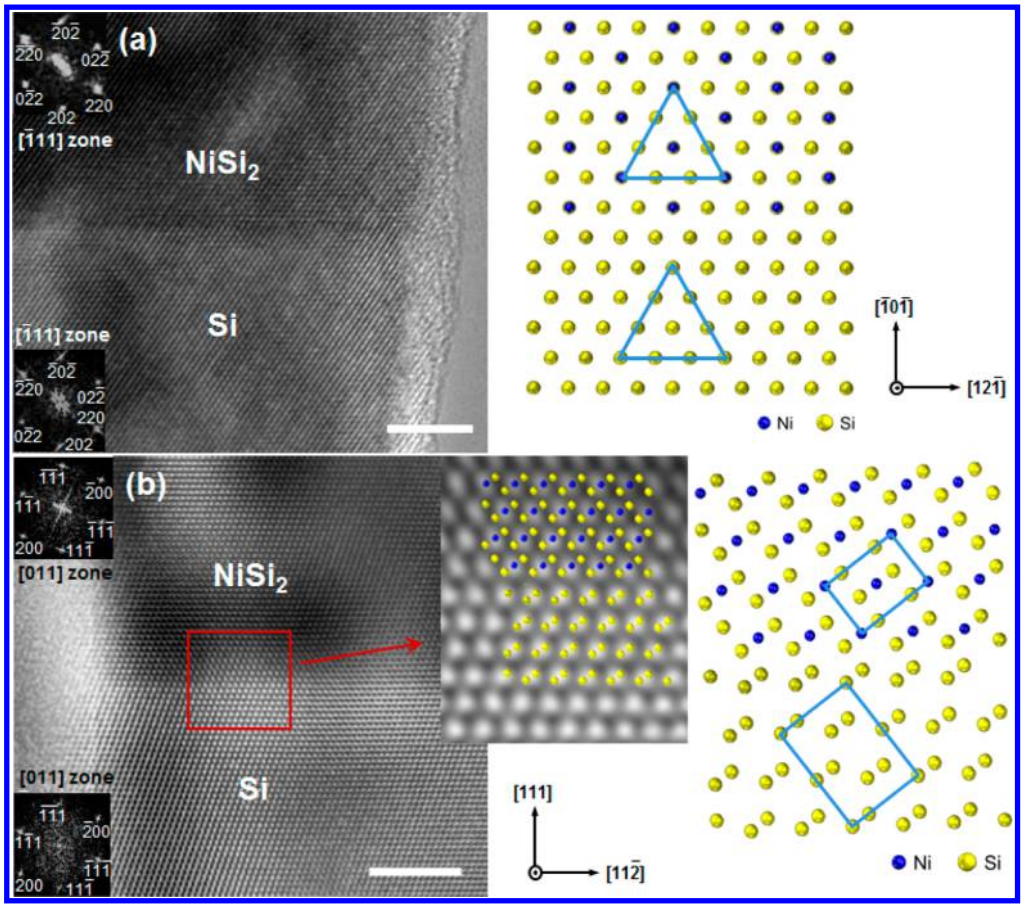

Figure 1. Post-growth HRTEM images and the simulated atomic arrangements of the interfaces of $NiSi_2$ and Si from two different nanowires with [110] in (a) and [111] in (b) orientations. The insets at the left are the fast Fourier transform (FFT) diffraction patterns of $NiSi_2$ (upper image) and Si (lower image). The conventional cubic unit cells are indicated in Si and $NiSi_2$ lattices at the schematic diagrams. The scale bars stand for 5 nm. (a) A post-growth lattice image with atomic arrangements of Ni and Si of a $NiSi_2$/Si heterostructure formed via point contact reaction between Ni nanoparticles and a [110] oriented Si nanowire at 750 °C. The viewing direction is 111 for Si and $NiSi_2$. The unit cells of $NiSi_2$ and Si are composed of three {111} planes as indicated by the blue lines that form triangular shapes. (b) A post-growth lattice image and schematic diagrams showing Ni and Si atomic positions in a $NiSi_2$/Si heterostructure formed via the point contact reaction between Ni nanopads and a [111] oriented Si nanowire at 400 °C. It is an A-type interface, where a twinning relation is shown. The viewing direction is 110 for Si and $NiSi_2$.

solutes,[32] the Ni dissolution has changed the state of the strain level in the Si lattice and influenced the kinetics of phase transformation. The phase transformation from Si to $NiSi_2$ includes the processes of repeating nucleation and stepwise atomic layer growth, and the generation and relaxation of strain is synchronized with the nucleation and growth. We show the direct correlation between strain level fluctuation and the atomic layer by atomic layer formation of $NiSi_2$ in a nanowire of Si. The silicide atomic layer forms by homogeneous nucleation and stepwise growth once the dissolved Ni atoms reach the required supersaturation level, yet the formation of the atomic layer silicide consumes the supersaturation of Ni atoms.

The depletion of the supersaturated Ni returns the strained-Si state. This is because the epitaxial misfit between $NiSi_2$ and Si (without Ni interstitials) generates tensile strain in Si but it is reduced locally during the dissolution of a supersaturated interstitial Ni. Yet the tensile strain in Si comes back once the process of the Si transformation to $NiSi_2$ occurs by consuming the supersaturated Ni atoms near the epitaxial interface. The generation and relaxation of strain is periodic with the atomic layer reaction. We propose a direct correlation between them, that is, the periodic strain level fluctuation results from the occupation and depletion of supersaturated Ni atoms in Si that enables the periodic homogeneous nucleation and growth of atomic layer of silicide in the Si nanowire.

In the heterostructure of $NiSi_2$/Si/$NiSi_2$, the competition of nucleation events of $NiSi_2$ on both sides of the Si nanogap should be considered, and we discuss here the probability of the nucleation events at the two interfaces. We note that the strain mapping on Ge and Si nanowires has been studied by high-resolution transmission electron microscopy (HRTEM) and geometric phase analysis.[33,34] In this paper we show in situ the silicide formation in Si nanowires in transmission electron microscope (TEM) and the local strain variation during $NiSi_2$ formation at the epitaxial silicide/Si interfaces. We address the real time cyclic strain effects as a dynamic process on the nucleation and growth events at the interface and correlate the observations with every nucleation event for $NiSi_2$ formation and discuss the thermodynamics of the chemical reactions.

Silicidation occurred in Si nanowires with [110] and [111] axial directions presents different atomic arrangements at the interfaces of $NiSi_2$ and Si with (110) and (111) planes.[28,31] They are shown in Figure 1a,b, respectively. Figure 1a shows the $NiSi_2$/Si heterostructure in atomic resolution in a [110] oriented Si nanowire, where the interface is atomically sharp with epitaxial relation of $NiSi_2[\bar{1}11]//Si[\bar{1}11]$ and

DOI: 10.1021/acs.nanolett.5b01234
Nano Lett. 2015, 15, 4121−4128

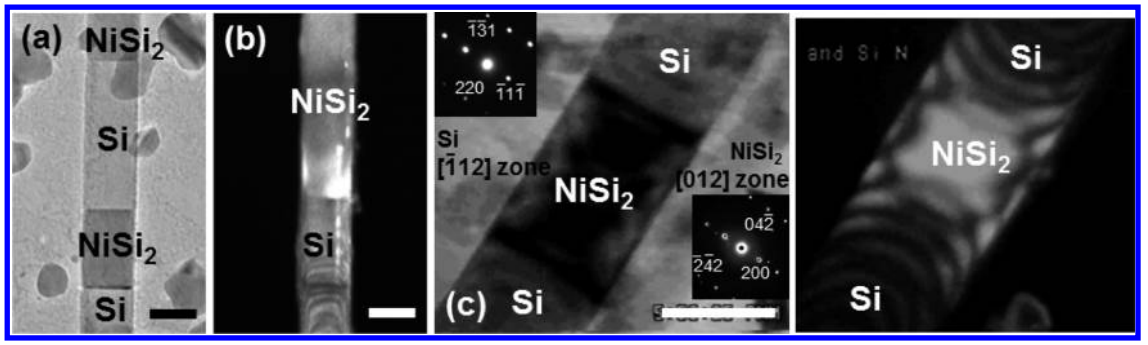

Figure 2. TEM images of $NiSi_2$/Si heterostructures during $NiSi_2$ formation in Si nanowires by point reactions at 777 °C. The scale bars are 50 nm. (a) A bright-field TEM image of a $NiSi_2$/Si multiple heterostructure in a Si nanowire. The gray dots beside the nanowire are Ni nanoparticles. (b) A dark-field TEM image at a $NiSi_2$/Si interface. It shows strain fringes in Si region are more obviously than in Si. (c) Stills from an in situ TEM movie of a Si/$NiSi_2$/Si heterostructure taken in bright-field (left side image) and dark-field (right side image) imaging modes that shows strain distribution in the heterostructure. The strain mainly accumulated in the Si region but spreads out to silicide due to the high strain magnitude. The insets show the diffraction patterns of Si (upper left) and $NiSi_2$ (lower right) where the viewing direction of Si is [211] and that of $NiSi_2$ is [210].

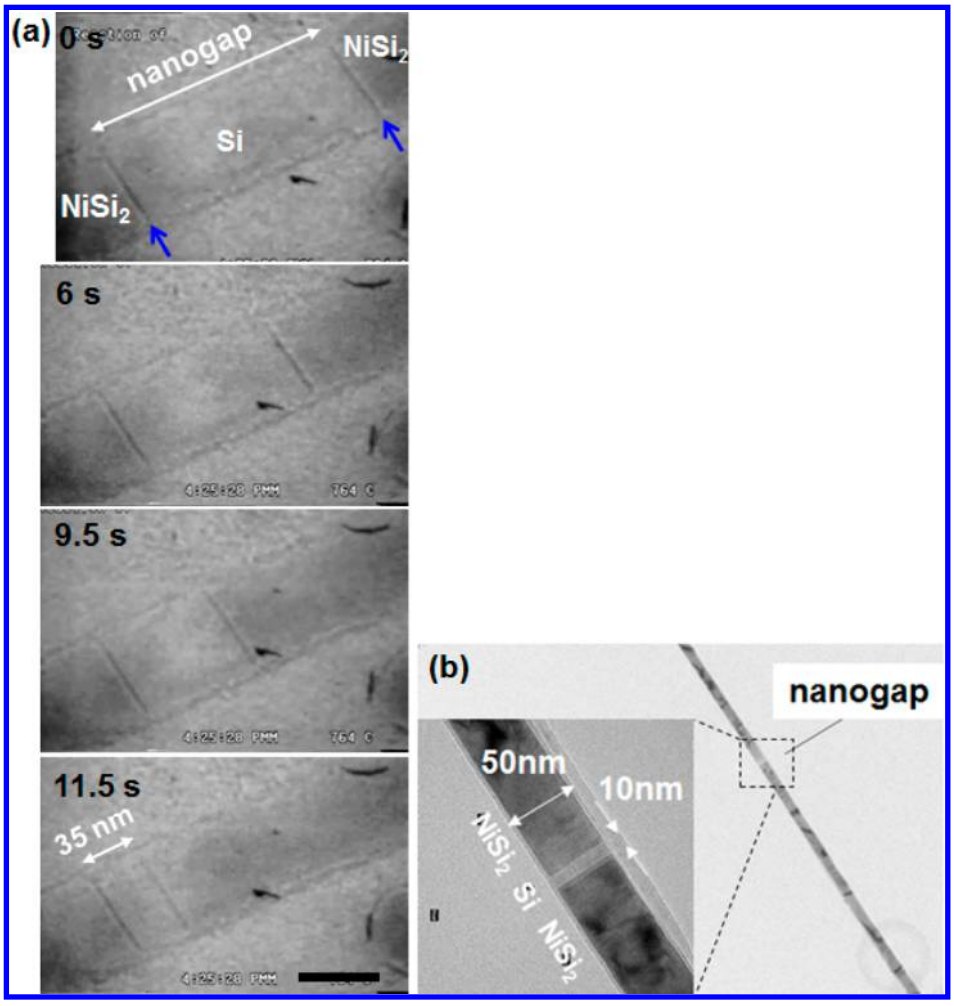

Figure 3. Epitaxial growth of $NiSi_2$ in a Si nanowire. (a) A sequence of TEM images of $NiSi_2$ formation at 764 °C in a Si nanowire by point contact reaction. The Si transformed to $NiSi_2$ and the middle Si segment became narrower with time from 0 to 11.5 s. The blue arrows indicate two $NiSi_2$/Si interfaces and the distance in-between indicates the width of the Si nanogap. The scale bar stands for 50 nm. (b) A Si nanogap with the width of 10 nm was formed during the reactions of a Si nanowire and two Ni nanopads at ~400 °C in in situ TEM. The images were taken after the sample was cooled down and stabilized at room temperature.

$NiSi_2(220)//Si(220)$. The HRTEM image and the simulated diagram show the good epitaxy owing to their close lattice parameters. Figure 1b shows the $NiSi_2$/Si heterostructure in atomic resolution, where the silicidation occurred in a [111] oriented Si nanowire with the epitaxial relation of $NiSi_2[011]//Si[011]$ and $NiSi_2(11\bar{1})//Si(11\bar{1})$. It is an A-type interface with 7-fold coordination of the Ni atoms closest to the interface. The silicidation occurs by homogeneous nucleation in single crystal [111] oriented Si nanowires,[31] whereas the silicide formation on [110] oriented Si nanowire can occur by either

DOI: 10.1021/acs.nanolett.5b01234
Nano Lett. 2015, 15, 4121−4128

Table 1. Parameters of $NiSi_2$, NiSi, Si, and Ni*

	a of Si	a of $NiSi_2$	Si (111)	$NiSi_2$ (111)	NiSi (311)	a of Ni
at RT	5.431 Å	5.416 Å	3.136 Å	3.121 Å	3.116 Å	3.524 Å
α ($°C^{-1}$)	2.6×10^{-6}	16.3×10^{-6}	2.6×10^{-6}	16.3×10^{-6}	40×10^{-6}	17.8×10^{-6}
at 630 °C	5.439 Å	5.469 Å	3.140 Å	3.152 Å	3.192 Å	3.562 Å

*a is the lattice constants of the crystals. α is thermal expansion coefficient.

homogeneous or heterogeneous nucleation[28] due to the lower surface energy and closely packed arrangement of Si atoms on (111) plane, which reflects different degrees of supersaturation for nucleation. The misfit strain at the interface of $NiSi_2$ and Si in both cases is calculated to be 0.46% at room temperature (RT) where Si is under compression due to the smaller lattice constant phase of $NiSi_2$. In addition, for practical use the strain at the interface is related to the charging under electric field that causes the changes of distances between atoms.[38]

In Figure 2, we show the distribution of strain fringes in the $NiSi_2$/Si heterostructure nanowires from in situ videos taken during reactions. Figure 2a shows a nanowire of $NiSi_2$/Si multiple heterostructures by point contact reactions of Ni nanoparticles and a Si nanowire at 777 °C under in situ control. Figure 2b shows another nanowire of $NiSi_2$/Si heterostructure at dark-field imaging condition where the fringes indicate the local strain field in the nanowire. The contrast in $NiSi_2$ is much more uniform than that in Si, whereas the Si segment contains contrast fringes which indicate strain distribution. This demonstrates that the strain caused by silicidation is mostly located in the unreacted Si region and the silicide is about strain-free or with low strain. Figure 2c shows a Si/$NiSi_2$/Si heterostructure in both bright-field and dark-field imaging conditions where a short $NiSi_2$ segment is formed in a Si nanowire. The bright-field image shows an overview of the heterostructure; whereas the dark-field image lights up the {110} planes and indicates the strain induced by the phase transformation from Si to $NiSi_2$. The strain is induced by the new phase, the short segment of $NiSi_2$, which acts as the center of the strain field and the strain distribution is symmetrical in the heterostructure. As different from the previous cases, the strain in this nanowire is expected to be large because of the much bigger lattice mismatch at the interface of Si {220} and $NiSi_2$ {042}. On the basis of the epitaxy and the DPs obtained from the experiment, the misfit at the interface was calculated to be 26% (without counting thermal expansion), which was very high so that the fringes in this case were significantly obvious in the dark-field TEM image (Figure 2c, the right side image). The smooth fringes in the dark-field image exhibit that the strain is highly elastic without plasticity such as dislocations. Yet the lattice constants of $NiSi_2$ and Si are similar, with the difference about 0.46%, and both of the phases have the same crystal structure so they typically form epitaxial interface with little strain. The image in Figure 2c is an extreme case to show the symmetrical distribution of strain with high elasticity in single crystal Si.

The formation of $NiSi_2$/Si/$NiSi_2$ heterostructures by point contact reactions is illustrated in Figure 3a where we show the captures from a movie recorded in TEM during the reactions. The $NiSi_2$ formation in the [111] oriented Si nanowire shows that the $NiSi_2$ grows with a sharp interface on Si, indicating an epitaxial growth. This attributes to the same cubic structure and close lattice parameters of $NiSi_2$ and Si, and it is consistent with our previous observations.[11] The strain in the Si nanowires was induced by volume change during phase transformation from Si to $NiSi_2$ by considering the total volume of the nanowire is finite due to native oxide coverage on the nanowire surface.[35−37] The $NiSi_2$/Si interfaces, as indicated by the arrows in Figure 3a, move toward the middle Si region with the rate of ∼10 nm/s at 764 °C. The width of the middle Si segment can be controlled down to a few nanometers in situ in TEM as shown in our previous publication[30,35] and Figure 3b. Figure 3b shows a post growth TEM image of $NiSi_2$ formed in a Si nanowire from the reactions between a Si nanowire and two Ni nanopads at ∼400 °C resulting in a heterostructure having a Si nanogap of 10 nm in width, embedded between two $NiSi_2$ segments. New phase formation causes strain in the matrix due to lattice mismatch and the relation is described by Poisson's ratio for isotropic materials. The Si nanowires used in the experiments were handled under non ultrahigh vacuum so the native oxide covering the Si nanowires is expected, which confines the shape of the nanowire. Therefore, the length of the nanowire stays without change where the strain generated by new phase formation is stored in the nanowires.[35] Because of the coverage of Si native oxide on the Si nanowire, the strain level in the Si nanogap is maintained during the new phase formation. It is worth mentioning that the native oxide on Si is protective, therefore the interface between Si and its oxide cannot serve effectively as source and sink of vacancies, and in turn there is no lattice shift to relax the strain during the reaction. We note that this is opposite to the classic Darken's analysis of interdiffusion, where there is no stress effect because lattice shift accommodates any volume strain under the condition of equilibrium vacancy everywhere in the sample.

Because the elastic strain could play a significant role in nucleating a new phase, we discuss below the implications of strain effect at the silicide/Si interface on nucleation and growth of the silicide.

At room temperature, the lattice constant of $NiSi_2$ is smaller than that of Si so the Si lattice near the interface is under compression, see Table 1. By considering thermal expansion during reactions at the reaction temperature, say 630 °C (903 K), the thermal expansion coefficients (α) and relative parameters of Ni, Si, and $NiSi_2$ are listed in Table 1.[39−42] It reflects that the lattice constant of $NiSi_2$ becomes larger than that of Si and the little expansion in Ni does not change the interstitial characteristics in Si at the reaction temperature. It makes the strain effect to be distinctive during the chemical reactions. Using Poisson's ratio

$$\nu = -\frac{\varepsilon_r}{\varepsilon_z}$$

where the axial direction of the nanowire is along z-axis, we assume the cross section of the nanowire is spherical and the radius is r. The lattice constant of $NiSi_2$ at 630 °C is larger than that of Si, so the Si lattice at the $NiSi_2$/Si interfaces in the direction parallel to the plane of interface (say the r-direction) is stretched by about 0.57%. Therefore, the Si lattice in the direction normal to the epitaxial interface (say the z-direction) is compressed up to 1.14%, which is the linear sum of the strain

DOI: 10.1021/acs.nanolett.5b01234
Nano Lett. 2015, 15, 4121−4128

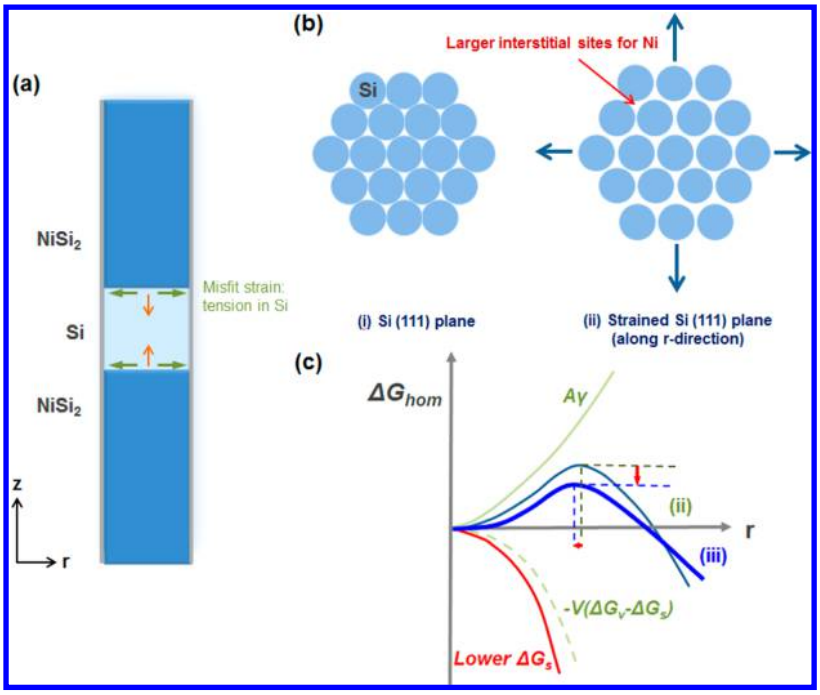

Figure 4. Schematic diagrams of a $NiSi_2/Si/NiSi_2$ heterostructure and its atomic arrangement at the cross section interfaces. (a) After phase transformation of a Si nanowire to a $NiSi_2/Si/NiSi_2$ heterostructure. The arrows indicate the directions of strain where the green arrows show the expansion of Si lattice caused by the misfit at $Si/NiSi_2$ interfaces at the reaction temperature and the orange arrows show the compression caused by the resistance of volume expansion by the native oxide confinement. (b) Atomic arrangement on Si (111) plane with (right) and without (left) strain. On the right-hand side one, it shows schematically the Si lattice near the interface and the interstitial sites expanded which provide larger sites for accommodating supersaturated interstitial Ni. (c) The variation of ΔG with r for homogeneous nucleation by taking account of tensile strain in Si lattice at the interface as in (ii) and after the supersaturation of Ni atoms fill up the interstitial sites as in (iii).

in r direction as illustrated in Figure 4a. This is in agreement with the assumption of a constant unit cell volume as in the calculation of Poisson's ratio in tension tests. When we dissolve a high supersaturation of Ni in Si, the interstitial Ni will expand the Si lattice, or we can say the Si is under compression because the Si atoms are squeezed. Because the Si lattice at the interfaces is under tension in the r-direction by misfit (Figure 4b), the interstitial Ni atoms will reduce the misfit strain at the interface between $NiSi_2$ and Si. Thus, the Si lattice in r-direction near the interface acts as "sinks" for Ni atoms so that a high degree of solubility of supersaturation of Ni can take place, which is needed in the homogeneous nucleation of a new layer of $NiSi_2$ on Si.

After the nucleation and growth of an epitaxial atomic layer of $NiSi_2$, the event has consumed the supersaturated Ni so the Si lattice is back to the initial state with misfit strain again but waiting to nucleate a new layer during another incubation period. As shown schematically in Figure 4a, Si lattice is under tension in r-direction by lattice misfit that tends to expand the nanowire radius, however, the Si nanowire does not have a free surface but rather a stable native oxide, which tends to resist the radial expansion of the Si nanowire, so the misfit strain accumulates in the Si lattice. The Si nanogap therefore is under compression in z-direction. The supersaturation of Ni solutes is supplied to the stretched Si lattices, as shown in Figure 4b, and release the misfit strain, as shown by the blue curve in Figure 4c (more details will be discussed below). Note that the supersaturation required for the homogeneous nucleation is about 1000.[31]

To study more broadly the strain effect during the epitaxial reaction, we take the case of NiSi formation in Si nanowires via point contact reaction[35] for comparison as NiSi has larger lattice misfit with Si which shows the strain effect more distinctly. NiSi forms an epitaxial interface with Si following $Si[1\bar{1}0]//NiSi[1\bar{1}2]$ and $Si(111)//NiSi(31\bar{1})$ and the corresponding parameters at the interface of NiSi and Si are listed in Table 1. The lattice misfits, indicating the degree of tensile strain at the interface of $NiSi(311)/Si(111)$ and $NiSi_2(111)/Si(111)$, are 1.65% and 0.38%, respectively. It demonstrates that higher lattice misfit results in higher tensile strain at the Si lattice, as shown in NiSi formation in Si nanowires, which provides more driving force for homogeneous nucleation and epitaxial growth to occur.

The nucleation events at both ends of a Si nanogap (e.g., Figure 3) are of interest because of their competition in nucleation; we ask which end will nucleate first in the atomic layer reaction? Typically, nucleation is kinetically a fluctuation phenomenon and occurs abruptly. Thus, either end should have equal probability to occur, provided that the microstructure of the nanogap is symmetrical. We expect the nucleation to be a random event on the both ends of the Si nanogap between two $NiSi_2$ segments. Once the nanogap has the supersaturation of Ni required for critical nucleus formation, it occurs on one side and depletes the supersaturation, so the other side cannot nucleate. However, the competition of the two nucleation events may be affected by the source of supply of Ni and the diffusion barrier when Ni atoms diffuse through Si and $NiSi_2$ segments in nanowires.

In Figure 5, we show the variation of the strain level during atomic layer reaction of $NiSi_2$ formation in a Si nanowire, which directly indicates the effect of strain on silicide formation. Figure 5a–e shows a sequence of dark-field TEM images during $NiSi_2$ formation in Si nanowires. The dark-field imaging, which shows the crystallinity directly, demonstrates that the electron

DOI: 10.1021/acs.nanolett.5b01234
Nano Lett. 2015, 15, 4121–4128

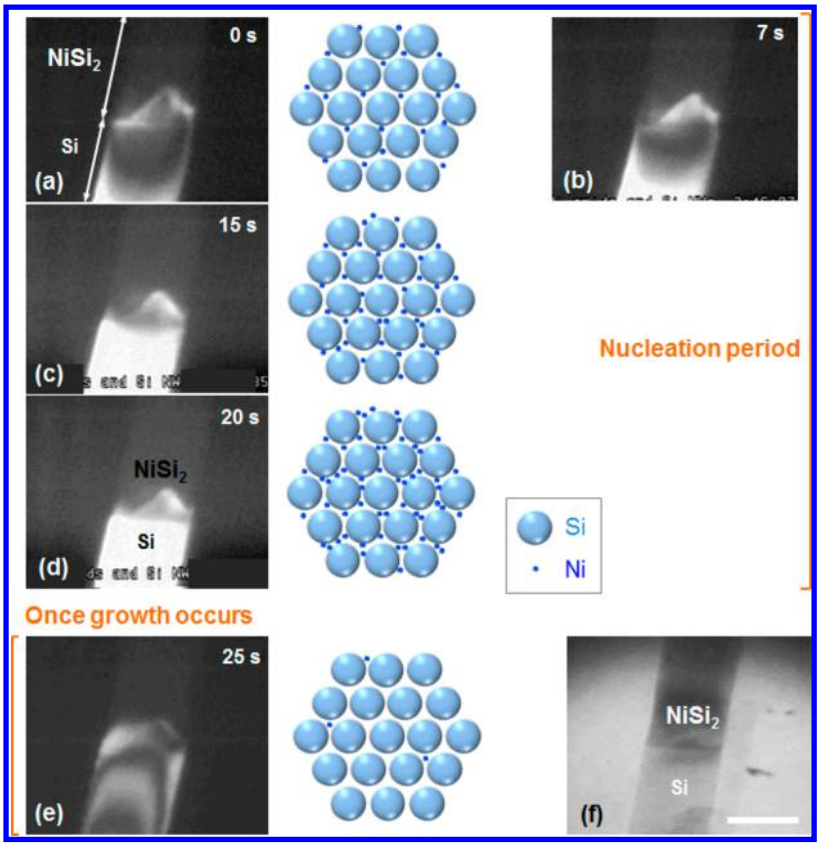

Figure 5. Sequence of in situ movie captures during $NiSi_2$ formation in a [111] oriented Si nanowire at 630 °C with schematic diagrams showing Si lattice at 111 interface with tensile strain and larger interstitial sites for Ni atoms. We note that the actual solubility of interstitial Ni is extremely small in Si, so the large number of the tiny dots, which represent the interstitial Ni atoms in the schematic diagram, is greatly exaggerated. (a–e) Dark-field images show the reaction from the nucleation period to the growth of one atomic layer of $NiSi_2$. The energy barrier at the initial state as in (a) and (e) is illustrated by (ii) in Figure 4c and the barrier goes lower as illustrated by (iii) in Figure 4c when Ni accommodates into the interstitial sites in strained-Si as in (d). The corresponding time is indicated on the images. (f) A bright-field image of the $NiSi_2$/Si heterostructure of the same nanowire after reaction. The scale bar is 50 nm.

beam diffraction conditions at the interface where $NiSi_2$ forms keeps varying during the reaction. It supports the kinetic processes of a repeating nucleation and growth at the epitaxial $NiSi_2$/Si interface. At the nucleation stage, it has tensile-strained-Si at the interface and starts with collecting Ni atoms at the relatively larger interstitial sites in Si lattice until the required amount of supersaturated Ni atoms is reached for homogeneous nucleation. Please also notice that it has compression in Si lattice along *z*-direction so the Ni atoms tend to accumulate along *r*-direction, which supports the fact that new layers grow along *r*-direction. Once it reaches the supersaturation of Ni required for nucleation, the Ni atoms will be quickly consumed to form a critical size of nucleus and followed by the radial growth of an atomic layer of $NiSi_2$ on Si matrix. During the incubation time, the strain is released by dissolving Ni atoms so that the gray contrast in Figure 5a shrinks and returns to flat interface, as shown in Figure 5a–d. Once the nucleation and growth start, which consumes the supersaturation of Ni, the Si is depleted of Ni and returns back to the strained-Si state as shown in Figure 5e. Figure 5f is a bright-field TEM image after reaction for comparison. As discussed above, the misfit strain between $NiSi_2$ and Si is more significant at higher temperatures. We expect that the growth rate speeds up at higher temperatures due to not only the faster diffusion but also the higher tensile-strain in Si lattice near the interface.

The phase transformation from Si to $NiSi_2$ in a nanowire may be regarded as a precipitation phenomenon, in which Ni atoms diffuse into Si lattices and transform to $NiSi_2$ when Ni reaches supersaturation to overcome the energy barrier of forming a nucleus of the new phase. It is homogeneous nucleation because of the low interfacial energy of native oxide and Si as compared to that of silicide and Si.[31] Given the total free energy change in homogeneous nucleation as

$$\Delta G_{\text{hom}} = -V\Delta G_{\text{v}} + A\gamma + V\Delta G_{\text{s}}$$
$$= -\pi r^2 a(\Delta G_{\text{v}} - \Delta G_{\text{s}}) + (\pi r^2 + 2\pi r a)\gamma$$

where $V\Delta G_{\text{v}}$ is a volume free energy reduction from a new phase with volume V, $A\gamma$ is a free energy increase from the new interface, and $V\Delta G_{\text{s}}$ is caused by misfit strain. This is shown as a function of nucleus radius in Figure 4c. The $(\Delta G_{\text{v}} - \Delta G_{\text{s}})$ is the driving force of the phase transformation where we note that the misfit strain energy is to reduce the effective driving force for forming a new phase. Specifically, in our case the supersaturated interstitial Ni releases the misfit strain and enhances the driving force of the chemical reaction. Taking into account of the strain energy, we found that the critical radius of nuclei is smaller and critical activation energy of forming $NiSi_2$ is lowered, as indicated by the arrows in Figure 4c. Besides, the increase of the Ni solute atoms makes a free energy gain due to the system entropy increases with the Ni atom diffusion into the Si matrix, so that thermodynamically it favors to form a new

DOI: 10.1021/acs.nanolett.5b01234
Nano Lett. 2015, 15, 4121–4128

phase. Thus, strain energy indeed affects the chemical driving force for the phase transformation.

The coherent strain energy in epitaxial growth has been analyzed by Cahn and Hilliard in spinodal decomposition.[43−45] There is no need to repeat the details here. Actually as a follow-up of the present study and more than just coherent strain energy, we need the gradient of stress potential to be the driving force for "uphill diffusion" of interstitial Ni atoms in Si to go to the epitaxial interface. We intend to report it separately.

Generally speaking, the strain level could also affect atom diffusion due to the effect of activated volume, but it is beyond the scope of study here. Furthermore, the distribution of strain in nanowires is also important in nanoscale phase transformations in core−shell nanowires, too.[46−49] The twinning formed in Si nanowires generate defects at the interface that changes the nucleation and growth events.[50] Defect releases strain at the interface that results in heterogeneous nucleation with a low degree of supersaturation. The strain effect in such nanostructures is of interests for future discussions.

In summary, we have shown the periodic variation of strain during the formation of epitaxial $NiSi_2$ in Si nanowires by point contact and atomic layer reactions. The atomic layer growth occurs periodically and the period depends on the incubation time of nucleation. The strain level and its periodic fluctuation near the interfaces of $NiSi_2$/Si heterostructures have been demonstrated in situ in TEM and the smooth strain fringes imply the high elasticity of the heterostructure. The Si lattice was under tensile strain due to the interfacial misfit whereas it was relaxed by the interstitial solution of supersaturated Ni atoms in the strained-Si lattice during the incubation time before each event of homogeneous nucleation. The strain relaxation occurred during the phase change of Si to $NiSi_2$ and it was observed to be periodic in synchronization with the nucleation event. The strain effect may be the reason that a high degree of supersaturation of Ni can take place near the interface. The strain level returns to the initial state once growth occurs. In addition, we believe that the effect of elastic strain on the growth kinetics and thermodynamics must be a general phenomenon regarding phase transformations in other similar nanoscale systems.

■ ASSOCIATED CONTENT

Supporting Information

Additional information on experimental details including material synthesis and selection of imaging modes in TEM. The Supporting Information is available free of charge on the ACS Publications website at DOI: 10.1021/acs.nanolett.5b01234.

■ AUTHOR INFORMATION

Corresponding Author

*E-mail: ycchou@nctu.edu.tw.

Notes

The authors declare no competing financial interest.

■ ACKNOWLEDGMENTS

We thank the support from the Ministry of Science and Technology of Taiwan under Grant NSC-101-2112-M-009-021-MY3 and the Center for Interdisciplinary Science under the MOE-ATU project for NCTU. The in situ experiment was performed at the Molecular Foundry at the Lawrence Berkeley National Laboratory, which is supported by the Office of Science, Office of Basic Energy Sciences of the U.S. Department of Energy under Contract No. DE-AC02-05CH11231.

■ REFERENCES

(1) Cress, C. D.; Datta, S. *Science* **2013**, *341*, 140−141.
(2) Lundstrom, M. *Science* **2003**, *299*, 210−211.
(3) Li, Y.; Qian, F.; Xiang, J.; Lieber, C. M. *Mater. Today* **2006**, *9*, 18−27.
(4) Mourik1, V.; Zuo1, K.; Frolov, S. M.; Plissard, S. R.; Bakkers, E. P. A. M.; Kouwenhoven, L. P. *Science* **2012**, *336*, 1003−1007.
(5) Lieber, C. M. *MRS Bull.* **2003**, *28*, 486−491.
(6) Ross, F. M. *Rep. Prog. Phys.* **2010**, *73*, 114501−114522.
(7) Samuelson, L. *Mater. Today* **2003**, *10*, 22−31.
(8) Chou, Y.-C.; Hillerich, K.; Tersoff, J.; Reuter, M. C.; Dick, K. A.; Ross, F. M. *Science* **2014**, *343*, 281−284.
(9) Gudiksen, M. S.; Lauhon, L. J.; Wang, J.; Smith, D. C.; Lieber, C. M. *Nature* **2002**, *415*, 617−620.
(10) Tomioka, K.; Yoshimura, M.; Fukui, T. *Nature* **2012**, *488*, 189−192.
(11) Jansen, R. *Nat. Mater.* **2012**, *11*, 400−408.
(12) Borg, M.; Schmid, H.; Moselund, K. E.; Signorello, G.; Gignac, L.; Bruley, J.; Breslin, C.; Kanungo, P. D.; Werner, P.; Riel, H. *Nano Lett.* **2014**, *14*, 1914−1920.
(13) Mann, R. W.; Clevenger, L. A.; Agnello, P. D.; White, F. R. *IBM J. Res. Dev.* **1995**, *39*, 403−417.
(14) Kittl, J. A.; Lauwers, A.; Chamirian, O.; Dal, M. V.; Akheyar, A.; De Potter, M.; Lindsay, R.; Maex, K. *Microelectron. Eng.* **2003**, *70*, 158−165.
(15) Weber, W. M.; Geelhaar, L.; Graham, A. P.; Unger, E.; Duesberg, G. S.; Liebau, M.; Pamler, W.; Chèze, C.; Riechert, H.; Lugli, P.; Kreupl, F. *Nano Lett.* **2006**, *6*, 2660−2666.
(16) Lavoie, C.; Detavernier, C.; Besser, P. Nickel silicide technology. In *Silicide Technology for Integrated Circuits*; The Institution of Engineering and Technology: London, U.K., 2009; p 102
(17) Maex, K. *Mater. Sci. Eng. R* **1993**, *11*, 53−153.
(18) Nava, F.; Tu, K. N. *Mater. Sci. R* **1993**, *9*, 141−200.
(19) Keyser, K. D.; Bockstael, C. V.; Meirhaeghe, R. L. V.; Detavernier, C.; Verleysen, E.; Bader, H.; Vandervorst, W.; Jordan-Sweet, J.; Lavoie, C. *Appl. Phys. Lett.* **2010**, *96*, 173503.
(20) He, Z.; Smith, D. J.; Bennett, P. A. *Phys. Rev. Lett.* **2004**, *93*, 256102.
(21) Higgins, J. M.; Ding, R.; Jin, S. *Chem. Mater.* **2011**, *23*, 3848−3853.
(22) Tung, R. T.; Gibson, J. M.; Poate, J. M. *Phys. Rev. Lett.* **1983**, *50*, 429−432.
(23) Peter, A. P.; Meersschaut, J.; Richard, O.; Moussa, A.; Steenbergen, J.; Schaekers, M.; Tőkei, Z.; Elshocht, S. V.; Adelmann, C. *Chem. Mater.* **2015**, *27*, 245−254.
(24) Schmitt, A. L.; Higgins, J. M.; Szczech, J. R.; Song, J. *J. Mater. Chem.* **2010**, *20*, 223−235.
(25) Wen, C.-Y.; Reuter, M. C.; Tersoff, J.; Stach, E. A.; Ross, F. M. *Nano Lett.* **2009**, *10*, 514−519.
(26) Stephan Hofmann, S.; Sharma, R.; Wirth, C. T.; Cervantes-Sodi, F.; Ducati, C.; Kasama, T.; Dunin-Borkowski, R. E.; Drucker, J.; Bennett, P.; Robertson, J. *Nat. Mater.* **2008**, *7*, 372−375.
(27) Chou, Y. C.; Lu, K. C.; Tu, K. N. *Mater. Sci. Eng. R.* **2010**, *70*, 112−125.
(28) Chou, Y. C.; Wu, W. W.; Li, C. Y.; Liu, C. Y.; Chen, L. J.; Tu, K. N. *J. Phys. Chem. C* **2011**, *115*, 397−401.
(29) Wu, Y.; Xiang, J.; Yang, C.; Lu, W.; Lieber, C. M. *Nature* **2004**, *430*, 61−65.
(30) Tang, W.; Dayeh, S. A.; Picraux, S. T.; Huang, J.; Tu, K. N. *Nano Lett.* **2012**, *12*, 3979−3985.
(31) Chou, Y. C.; Wu, W. W.; Chen, L. J.; Tu, K. N. *Nano Lett.* **2009**, *9*, 2337−2342.
(32) Bonzel, H. P. *Phys. Status Solidi* **1967**, *90*, 493.

DOI: 10.1021/acs.nanolett.5b01234
Nano Lett. 2015, 15, 4121−4128

(33) Taraci, J. L.; Hÿtch, M. J.; Clement, T.; Peralta, P.; McCartney, M. R.; Drucker, J.; Picraux, S. T. *Nanotechnology* **2005**, *16*, 2365−2371.
(34) Glas, F. *Phys. Rev. B* **2006**, *74*, 121302.
(35) Lu, K. C.; Wu, W. W.; Wu, H. W.; Tanner, C. M.; Chang, J. P.; Chen, L. J.; Tu, K. N. *Nano Lett.* **2007**, *7*, 2389−2394.
(36) Chou, Y. C.; Wu, W. W.; Cheng, S. L.; Yoo, B. Y.; Myung, N.; Chen, L. J.; Tu, K. N. *Nano Lett.* **2008**, *8*, 2194−2199.
(37) Wu, W. W.; Lu, K. C.; Wang, C. W.; Hsieh, H. Y.; Chen, S. Y.; Chou, Y. C.; Yu, S. Y.; Chen, L. J.; Tu, K. N. *Nano Lett.* **2010**, *10*, 3984−3989.
(38) Mamatkulov, M.; Filhol, J.-S. *J. Phys. Chem. C* **2013**, *117*, 2334−2343.
(39) Kollie, T. G. *Phys. Rev. B* **1977**, *16*, 4872−4881.
(40) Okada, Y.; Tokumaru, Y. *J. Appl. Phys.* **1984**, *56*, 314−320.
(41) Smeets, D.; Vanhoyland, G.; D'Haen, J.; Vantomme, A. *J. Phys. D: Appl. Phys.* **2009**, *42*, 235402.
(42) Detavernier, C.; Lavoie, C.; d'Heurle, F. M. *J. Appl. Phys.* **2003**, *93*, 2510−2515.
(43) Cahn, J. W. *Acta Metall.* **1961**, *9*, 795.
(44) Hilliard, J. E. In *Phase Transformations*; Aaronson, H. I., Ed.: ASM: Metals Park, OH, ; Chapter 12, p 497.
(45) Tu, K. N.; Gusak, A. M. In *Kinetics in nanoscale materials*; Wiley: New York, 2014; Chapter 5, p 131.
(46) Chou, Y. C.; Tu, K. N. In *One-Dimensional Nanostructures: Principles and Applications*; Zhai, T., Yao, J., Ed.; John Wiley & Sons, Inc.: Hoboken, New Jersey, 2013; Chapter 5.
(47) Lin, Y. C.; Chen, Y.; Xu, D.; Huang, Y. *Nano Lett.* **2010**, *10*, 4721−4726.
(48) Ogata, K.; Sutter, E.; Zhu, X. *Nanotechnology* **2011**, *22*, 365305.
(49) Liu, N.; Lu, N.; Yao, Y.-X.; Li, Y.-R.; Wang, C.-Z.; Ho, K.-M. *J. Phys. Chem. C* **2011**, *115*, 15739−15742.
(50) Tang, W.; Picraux, S. T.; Huang, J. Y.; Gusak, A. M.; Tu, K. N.; Dayeh, S. A. *Nano Lett.* **2013**, *13*, 2748−2753.

DOI: 10.1021/acs.nanolett.5b01234
Nano Lett. 2015, 15, 4121−4128